Separation Science and Technology
Publication details, including instructions for authors and subscription information:
http://www.informaworld.com/smpp/title~content=t713708471

Effect of Pressure on the Aging of Dense (PPO) Membranes

Alsdeg Alsari[a]; B. Kruczek[a]; T. Matsuura[a]
[a] Department of Chemical Engineering, University of Ottawa, Ottawa, Ontario, Canada

To cite this Article Alsari, Alsdeg , Kruczek, B. and Matsuura, T.(2007) 'Effect of Pressure on the Aging of Dense (PPO) Membranes', Separation Science and Technology, 42: 12, 2567 — 2582
To link to this Article: DOI: 10.1080/01496390701515169
URL: http://dx.doi.org/10.1080/01496390701515169

Separation Science and Technology, 42: 2567–2582, 2007

ISSN 0149-6395 print/1520-5754 online
DOI: 10.1080/01496390701515169

Effect of Pressure on the Aging of Dense (PPO) Membranes

Alsdeg Alsari, B. Kruczek, and T. Matsuura
Department of Chemical Engineering, University of Ottawa, Ottawa, Ontario, Canada

Abstract: The effect of gas pressure on membrane aging was studied thoroughly by applying feed gas pressure continuously or by reducing the feed gas pressure intermittently. Resemblance of aging curves of gas separation membranes to visco-elastic response curves was observed for all the studied membranes. Membrane aging curves consist of elastic and viscous components. It was further concluded that the elastic component of polymer relaxation was enhanced when membranes were aged at lower pressures while the viscous component was enhanced at higher gas pressures. The transition from the elasticity dominant to the viscosity dominant region occurred more quickly for thicker membranes.

Keywords: Membrane gas separation, aging, polyphenylene oxide, dense membrane, viscoelasticity

INTRODUCTION

Considering that most membranes for gas separation are prepared from glassy polymers, which like all glassy materials are subject to physical aging, the problem in predictability of membrane performance and its change with time should not be surprising. What is surprising, however, is the fact that although the phenomenon of physical aging of glassy polymers was recognized more than half a century ago, it was only in the mid 1990s when its importance was realized in the field of polymeric gas separation

Received 1 March 2007, Accepted 8 May 2007
Address correspondence to Alsdeg Alsari, Department of Chemical Engineering, University of Ottawa, 161 Louis Pasteur, Ottawa, Ontario, Canada. Tel.: 1-613-562-5800 (x6114); Fax: 1-613-562-5172; E-mail: saddegalsari@yahoo.com

membranes. Even with this realization, the research effort has been mostly focused on utilization of gases as a probe to study physical aging in glassy polymers. This is because physical aging is associated with changes in free volume and since the performance of gas separation membranes strongly depends on the free volume, it represents a fairly sensitive tool to monitor this phenomenon. On the other hand, no advantage was taken of this parameter, physical aging, to understand the molecular mechanism of gas transport through glassy polymers.

Gas separation membrane processes together with ultrafiltration, microfiltration, and reverse osmosis are classified as pressure driven processes. That means that the total or partial pressure difference between the two sides of the membrane is the driving force for the permeation of fluid components through the membrane. In gas separation, the gas pressure or concentration gradient should result in the permeation of gases through the membrane. The efficiency of a membrane gas separation process is exclusively characterized by the permselectivity of gases through the membrane. Gases will be separated on the basis of the difference in their permeation rates.

Physical aging is a change in all physical properties of glassy polymers with time to reach the corresponding equilibrium glassy state. As it is the most important parameter that affects the gas permselective properties of glassy polymers, the excess free volume is in the origin of the non-equilibrium state of these polymers. Physical aging is probed by the permeability of gases through glassy polymeric membranes. The free volume is quantitatively related to the permeability, P, by the following equation:

$$P = A \exp(-B/FFV) \tag{1}$$

A and B are constants and FFV is the fractional free volume which is defined as:

$$FFV = (v - v_o)/v \tag{2}$$

where v is the specific volume of polymer and v_o is the volume occupied by polymer chains.

Alfrey et al. proposed a qualitative model for the excess free volume relaxation in glassy polymers (1). According to the proposed mechanism, the excess free volume in glassy polymers exists in a form of mobile free volume holes, which can divide or combine, i.e. their individual identity is not necessarily preserved. As long as the holes remain within the sample, the free volume of polymer is unchanged. However, once the holes reach the surface of the sample, they disappear and the free volume of polymer decreases. This mechanism for the free volume relaxation has been referred to as free volume diffusion in glassy polymers (Fig. 1).

Kauzmann objected to the general notion of diffusion of free volume (2), and Hirai and Eyring proposed an alternative model in which they explained relaxation of the excess free volume in glassy polymers by a lattice contraction mechanism (3) (Fig. 2).

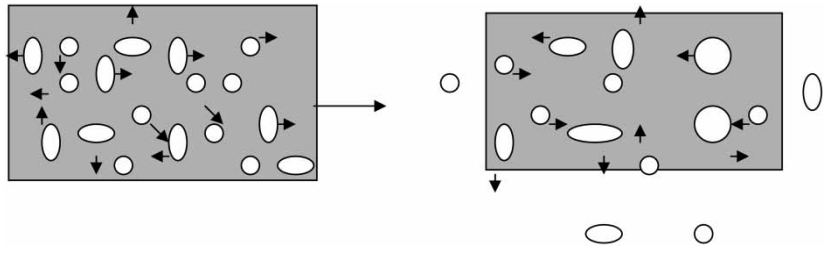

Figure 1. Schematic representation of free volume existence in polymeric film and its reduction by diffusion from the surfaces.

The authors suggested that the free volume (v_f) changes with time (t) according to the following equation

$$v_f = v_{f2} + (v_{f1} - v_{f2}) \exp(-t/\tau\beta) \tag{3}$$

where v_{f1} and v_{f2} are the initial and the equilibrium free volume, respectively, τ is a material relaxation time, and β is a dimensionless correction factor.

Curro et al. argued that lattice contraction could be coupled with free volume diffusion to describe the overall volume reduction upon aging (4). They proposed a quantitative analysis for the diffusion of the free volume holes limited by chain segmental motion, in which they described the change in the fractional free volume using Fick's second law of diffusion. They also proposed that the diffusion coefficient for the free volume holes should be correlated with the fractional free volume via a Dolittle-type equation.

The physical aging process, which refers to the structural relaxation toward equilibrium, is the continuation of the changes that take place at the glass transition temperature T_g. Glass transition is, by tradition, described as a reduction in segmental mobility due to temperature reduction. This may occur even at a temperature above T_g, when an increase in pressure or concentration of the system is applied. Thus, a glass transition pressure (p_g) would be defined by the freezing of the molecular motion, or the isobarial relaxation in free volume at a pressure higher than (p_g) (5). However, there is scarcity of information concerning the pressure dependence of dynamical quantities in

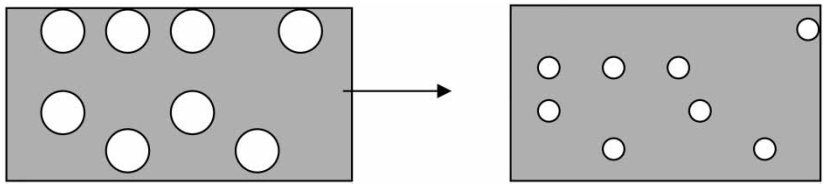

Figure 2. Schematic representation of the reduction of free volume by lattice contraction mechanism.

the glass transition regime, especially where the relaxation times depend strongly on the instantaneous state of the system (6). This is not the case in polymeric membranes for gas separation, where the process is driven by the pressure difference across the membrane, which places those membranes under pressure throughout the time of application.

Mechanical stresses have a strong effect on aging. Applying a stress before, during, and after aging leads to an acceleration of the aging, retardation, and a de-aging effect, respectively (7). Qualitative observations due to rapid changes of pressure were found to be similar to those obtained at atmospheric pressure by rapid changes in temperature (8). Quantitative studies by Deng and Jean on the effect of pressure using positron annihilation lifetime spectroscopy found that the free volume and free volume distribution decreased by increasing the pressure (9). Other researchers criticized those studies due to extraordinary decrease in the free volume caused by small changes in pressure (5).

In glassy polymeric membranes used for gas separation, there are not enough studies on the effect of pressure on the physical aging of glassy polymers. Some examples are the results of Pfromm and Koros (10) that show acceleration of aging, when the gas pressure is reduced. McCaig and Paul (11) carried out one experiment to study the effect of gas pressure. They compared the aging time for a 0.74 μm membrane aged under vacuum with that for a 0.58 μm film aged under operating gas pressure in a constant pressure system, and concluded that changing the operating conditions did not influence the aging response; i.e., the gas pressure or the used system had no effect on physical aging. This is opposite to what was concluded earlier by Pinnau et al. (12) that, the details of how permeation rates were measured could influence the observed aging. Nagai et al. (13) and Morisato et al. (14) have found out that aging was faster in constant volume system and suggested that contamination of a sample by the oil vapors in constant-volume systems with oil-lubricated vacuum pumps might have led to very significant overestimation of the extent of physical aging. Chung and Teoh discussed the effect of spinning rate on the aging of hollow fibers (15). Zhou et al. mathematically related the aging of thin and thick membrane terms of permeability decrease with time (16).

The objective of this paper is therefore to make a more thorough study of the aging of gas separation membranes, especially on the effect of the gas pressure on membrane aging. It is also attempted to interpret the gas permeation data based on the concept of mechanical stress-strain relationship such as visco-elasticity of the glassy polymer.

EXPERIMENTAL

Membrane Preparation

The method of membrane preparation was described in our earlier work. Briefly, a 1wt% solution of polyphenylene oxide (PPO) (T_g of 212°C and

average molecular weight M_w of 40,000) in trichloroethylene (TCE from Aldrich) was poured into a stainless steel ring fixed on a precisely leveled glass plate. The solution was left overnight, approximately 12 hours, for solvent evaporation, before the glass plate, together with the cast solution film, was immersed into a water bath for a short period until the membrane peeled off the glass plate spontaneously. Since the surface of the membrane was wetted in the water bath, the membranes were further dried in ambient air for either 6 or 16 hours in a free-standing position, before being mounted to the permeation cells. The moment when the membrane was mounted to the permeation cell and the feed gas pressure was raised to a set value for the measurement of the permeation rate is defined as time $t = 0$, even though physical aging started before $t = 0$.

All membranes are specified in Table 1, together with the details of the experiments for which the membranes were used.

Gas Permeation Experiments

Since the permeability coefficient is directly proportional to the gas permeation rate, the changes in the permeability coefficient due to the physical aging of the investigated membranes will be expressed on the basis of the changes in gas permeation rates. Moreover, to facilitate the comparison of the extent of the physical aging in different membranes, a dimensionless

Table 1. Membranes and gas permeation experiment details

Membranes				Experiments		
Used in figure	Number	Thickness (μm)	Drying time (h)	System	Routine	Feed pressure (psig)
Figure 4	4-A	3.9	16	CP	Continuous	25
	4-B	3.9	16	CP	Non-cont.	25
Figure 5	5-A	5.5	6	CP	Continuous	25
	5-B	5.5	6	CP	Non-cont.	25
Figure 6	6-A	7.25	6	CP	Continuous	25
	6-B	7.25	6	CP	Non-cont.	25
Figure 7	7-A	3.9	16	CP	Continuous	50
	7-B	3.9	16	CP	Continuous	25
Figure 8	8-A	5.5	16	CP	Continuous	50
	8-B	5.5	16	CP	Continuous	25
Figure 9	9-A	18	16	CP	Continuous	100
	9-B	18	16	CP	Non-cont.	100
Figure 10	10-A	15	16	CV	Continuous	100
	10-B	15	16	CV	Non-cont.	100

permeation rates, Q/Q_0, will be used, where Q_0 is the gas permeation rate immediately after installing a membrane inside the testing cell, i.e., at $t = 0$.

In this work two setups for gas permeation experiments were used. One is an automated multi-cell sweep-gas constant pressure system, abbreviated as the C-P system hereafter, and the other is a constant volume system, abbreviated as a C-V system hereafter. Both systems are briefly outlined below.

Automated Multi-cell Sweep-gas Constant Pressure System and Permeation Data Acquisition (C-P System)

The method used to measure the gas permeation rate is also known as the carrier gas method (17). It involves sweeping the permeated gas, normally at 1 atmospheric pressure, and routing it to be analyzed for the fluxes of each penetrant. The technique employs a gas chromatograph (GC) as the selective detector for monitoring the variation in gas concentration, as the gases permeate through the membrane (Fig. 3).

In this work, the feed stream (F) was air and the sweep stream (S) was methane. However, the system could also be used for other mixtures as well as for single gas permeation tests. The flow rate of the stream (S) is controlled by a mass flow controller (MFC), while the flow rate of the retentate (R) and thus the feed stream (F) is controlled by a needle valve (NV) in conjunction with a mass flow meter (MFM1). The flow rate of the permeate + sweep gas stream (PS) is monitored by another mass flow meter (MFM2). All mass flow meters and mass flow controllers are from the MKS company and have a detectable range from $0 - 10 \pm 0.1\ \text{cm}^3/\text{s}$. The present set-up employs an in-line sampling technique for the gas sample, followed by subsequent injection into a gas chromatograph for the composition analysis. The set-up is constructed with 316 stainless steel tubing and fittings for high pressure feed studies (0 to 500 psia). The entire set-up is automated for unsupervised operation by employing controller cards for the solenoid

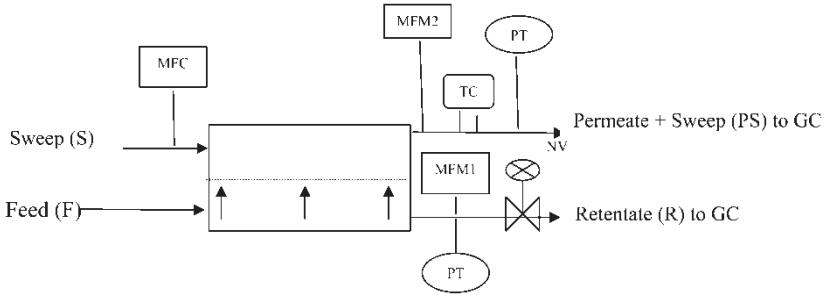

Figure 3. Schematic diagram of sweep gas constant pressure system.

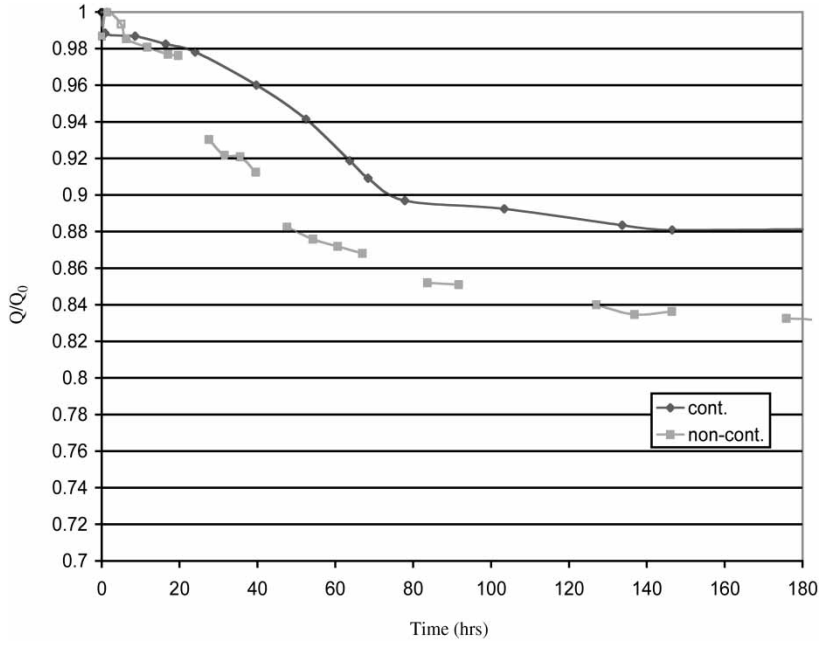

Figure 4. The change in the relative permeation rate with time. Membrane thickness, 3.9 μm; system, constant pressure system; feed pressure, 25 psig.

valve operation and data acquisition cards for pressure transducer (PT), thermocouple (TC) and mass flow meter readings.

The permeation rate of the *i* th gas species (either oxygen or nitrogen), Q_i, is evaluated from the flow rate of the PS stream (Q_{PS}) and its composition by

$$Q_i = x_{i,PS} Q_{PS} \tag{4}$$

where $x_{i,PS}$ is the mole fraction of the *i*-th species in the (PS) stream. It is important to mention that because of some back permeation of the sweep gas the total permeation rate of oxygen and nitrogen (ΣQ_i) was always slightly greater than the difference between the flow rates of the (PS) and (S) streams ($Q_{PS} - Q_S$). But this difference was negligible.

Constant Volume System (C-V System)

Another set-up for the gas permeation experiments is a constant volume system. The details of the system are given elsewhere (18). Briefly, the gas permeation rate is determined by monitoring the rate of pressure change on the permeate side, the total volume of which is maintained constant. Hence, it is called constant volume system. According to this technique, the total

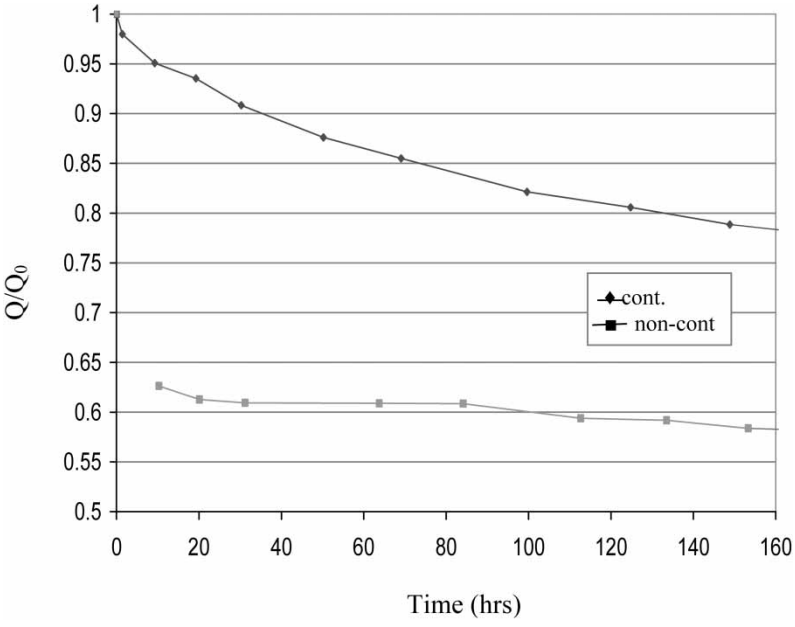

Figure 5. Effect of experimental scenario on the relative permeation rate. Membrane thickness, 5.5 μm; system, constant pressure system; feed pressure, 25 psig.

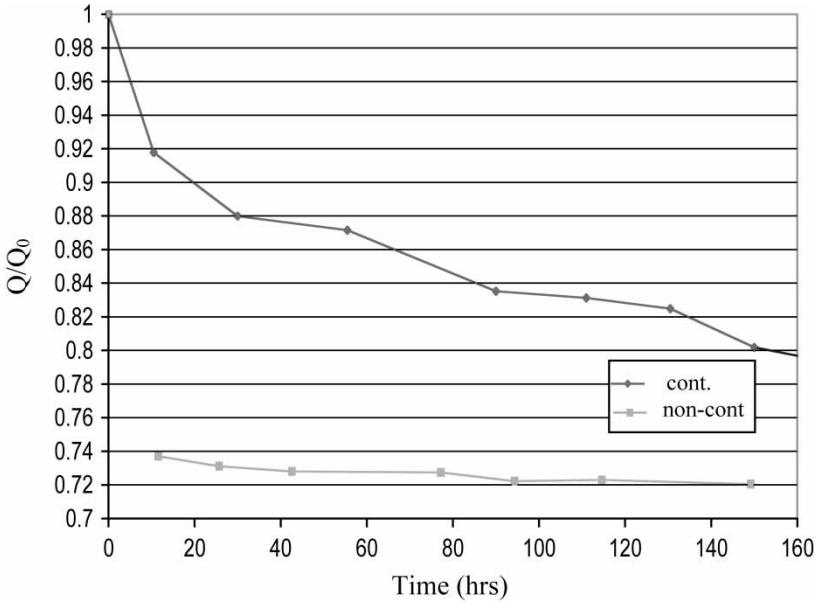

Figure 6. Effect of experimental scenario on the relative permeation rate. Membrane thickness, 7.25 μm; system, constant pressure system; feed pressure, 25 psig.

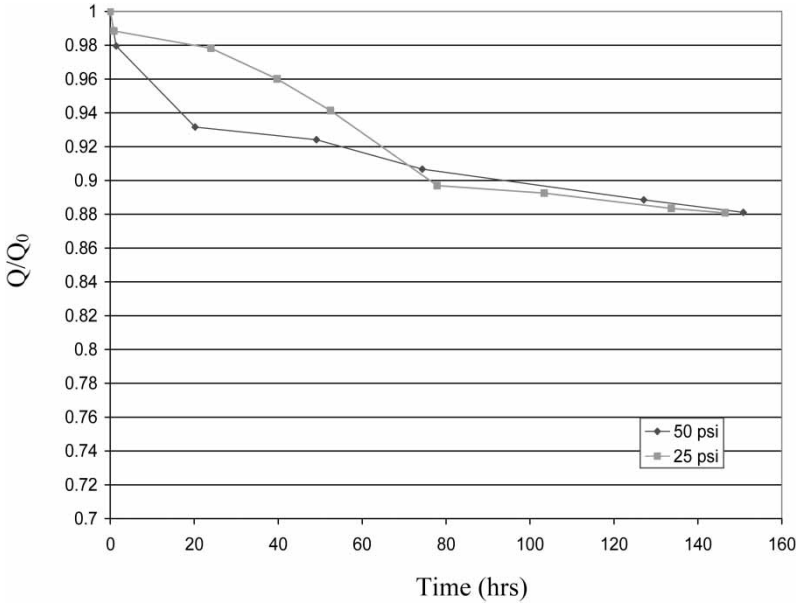

Figure 7. Effect of feed gas pressure on the relative permeation rate. Membrane thickness, 3.9 μm; system constant pressure system.

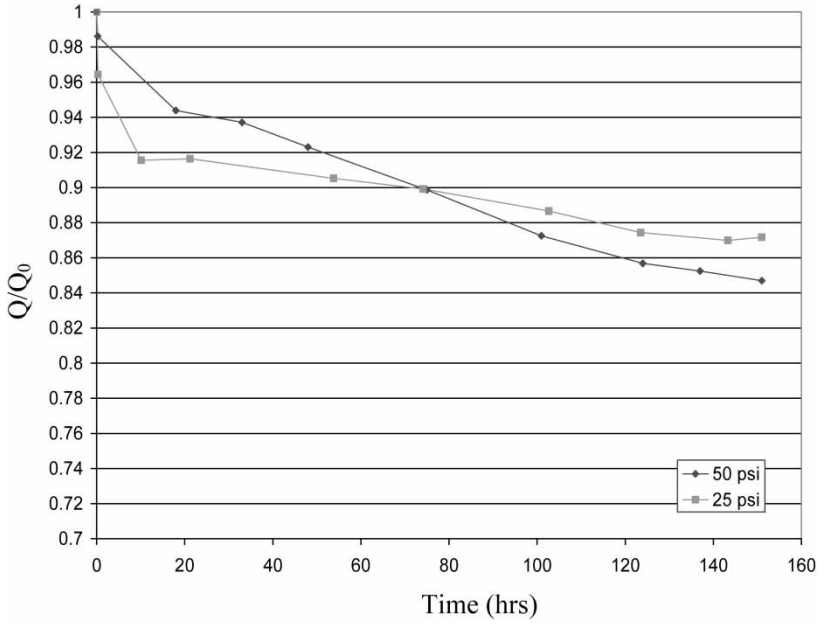

Figure 8. Effect of feed gas air pressure on the relative permeation rate. Membrane thickness, 5.5 μm; system, constant pressure system.

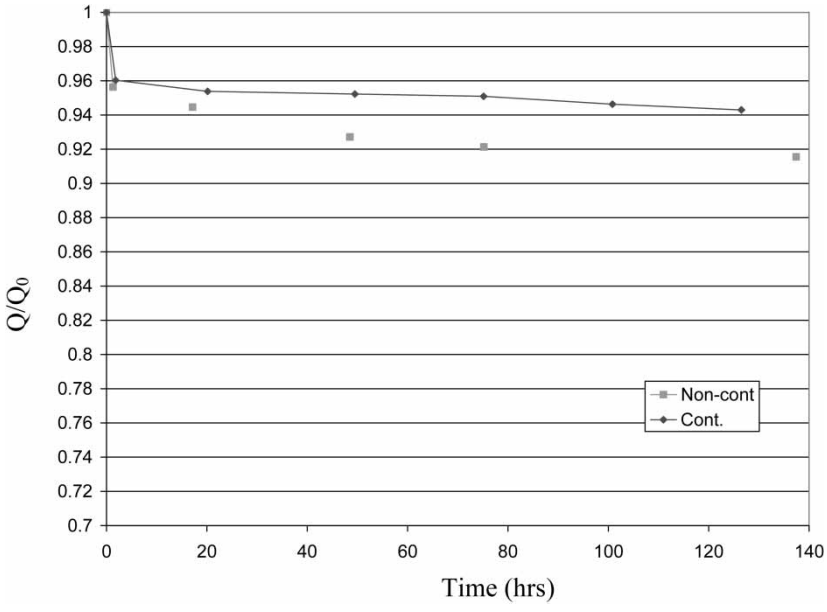

Figure 9. Effect of experimental scenario on the relative permeation rate. Membrane thickness, 18 μm; system, constant pressure system; feed pressure, 100 psig.

permeation rate, Q (cm^3 (STP)), is calculated by assuming the ideal gas behavior of the gas. Hence,

$$Q = (V/RT)(dp/dt) \tag{5}$$

where V is the total volume on the permeate side (cm^3), R is universal gas constant (62,356 cm^3 mmHg/mol K), T is the absolute temperature (K), and dp/dt is the rate of the pressure increase on the permeate side (mmHg/s).

Two operational routines

For both permeation systems two different operational routines, respectively called continuous routine and non-continuous routine, were applied. In the continuous routine, the membrane was under the normal operational conditions of gas permeation system throughout the experiment without any interruption; i.e., the membrane was always under the feed gas pressure on the feed side, while the permeate side was facing either the sweep gas stream at atmospheric pressure (C-P system) or vacuum (C-V system).

In the non-continuous routine, the normal operational condition was interrupted from time to time by exposing both sides of the membrane either to an atmospheric environment (C-P system) or to vacuum (C-V system). Since the

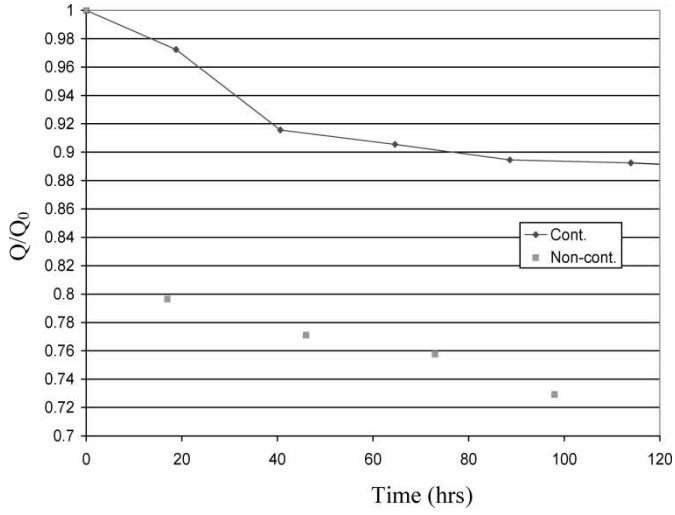

Figure 10. Effect of experimental scenario on the relative permeation rate. Membrane thickness, 15 μm; system, constant volume system; feed pressure, 100 psig.

pressure on the feed side was decreased from the operating pressure to either atmospheric pressure or to vacuum, this period of interruption is called "period of pressure reduction." This period is indicated by blank spaces where the data points are unconnected in Figs. 4–10.

The systems used, feed gas pressures, and the operational routines are given in Table 1 together with the membranes used for each experiment.

EXPERIMENTAL RESULTS

In Fig. 4, the relative permeation rate, Q/Q_0, is plotted versus operational period for two experiments (using membranes 4-A, 4-B) conducted with the C-P system. The two membranes used in these experiments had the same thickness, 3.9 μm, and the drying time in ambient air was 16 hours. In the figure, Q is the total, including oxygen and nitrogen, permeation rate at a time $t(\Sigma Q_i)$, while Q_0 is the total permeation rate at $t = 0$. Both membranes were under the feed gas pressure (25 psig) during the first 20 hours. In one experiment (4-A, continuous routine) the continuous routine was maintained throughout the experiment, while in the other experiment (4-B, non-continuous routine), there were several pressure reduction periods, that followed the first 20 hours of operation under pressure. Figure 4 shows that the aging rate is similar in both experiments during the first 20 hours. After this first stage of

operation, the permeation rate decreases almost linearly in the continuous routine, but the slope of decline changes after 80 hours. In the non-continuous routine, on the other hand, the permeation rate decreases more steeply during the pressure reduction periods, particularly when the operational period is shorter than 50 hours. However, the slope of decline diminishes and the line becomes almost parallel to the continuous routine in the later stage of the permeation experiment.

Figure 5 shows the permeation rate data from another two sets of experiments. Two membranes of the same thickness (5.5 μm) were used. Both membranes were dried for 6 hours. One experiment (with membrane 5-A) was performed following the continuous routine for 160 hours, while in the other experiment (with membrane 5-B) there was a pressure reduction period of 10 hours in the very beginning. Then, the feed pressure was applied. Figure 6 shows the results from the same experiments as Fig. 5 except for the membrane thickness that was 7.25 μm. In both figures, we can observe that the reduction in the permeation rate that occurred during the first 10 hours of non-continuous routine (with membranes 5-B and 6-B) is so severe that the experiments with the continuous-routine (with membranes 5-A and 6-A) do not reach that level of flux reduction even after 160 hours. We can also observe that the thinner membrane (5-B) is subject to a higher degree of flux reduction than the thicker (6-B) membrane.

In Fig. 7, the relative permeation rate, Q/Q_0, is plotted versus the operational period for two experiments (with membranes 7-A, 7-B) conducted with the C-P system under the air pressure of 50 and 25 psig, respectively. The two membranes used in these experiments had the same thickness, 3.9 μm, and the drying time in ambient air was 16 hours. The decrease in the relative permeation rate of about 12% was reached for both membranes at the end of the operation. The curves representing both experiments (7-A and 7-B) can be divided into two parts, i.e. the earlier sharp drop in the permeation rate followed by a less steep decline. Figure 8 shows the results from the same experiments except for the membrane thickness that was 5.5 μm. The final decline in the relative permeation rates are around 13% and 15% for operating pressure of 25 and 50 psig, respectively.

In Fig. 9, the relative permeation rate, Q/Q_0, is plotted versus the operational period for two experiments (with membranes 9-A, 9-B) conducted using the C-P system. The thickness of both membranes was 18 μm and the membranes were dried in ambient air for 16 hours before being mounted to the permeation cell. In both experiments, feed gas pressure (100 psig) was applied during the first hour and a half of the permeation test. During this period of operation, the loss in permeation rate was about 4% for both the membranes. After this early stage of operation, the continuous routine was maintained throughout the experiment for the membrane 9-A (continuous routine). On the other hand, in the other experiment (9-B, non-continuous routine), the gas permeation experiment was interrupted by long periods of pressure reduction. It is evident that the permeation rate decline decreased

significantly after the initial 1.5 hours of operation in both routines. Figure 10 shows similar experimental results from the C-V system; i.e., one experiment was conducted following the continuous routine (10-A) throughout the experiment while another set of experiments followed the non-continuous routine (10-B) with several long pressure reduction periods. The relative permeation rates are reported in this figure. While, in the continuous routine, the loss in the relative permeation rate was a little more than 10.5% after more than 100 hours of operation, in the non-continuous routine the loss in the relative permeation rate reached about 27% after 98 hours of operation. Interestingly, 20% of the loss occurred during the first 20 hours of operation.

DISCUSSION

Physical aging essentially affects the relaxation times. Relaxation time is not a single value, but a distribution of values that change with experimental time. Relaxation times calculated using mathematical relations, as in Eq. (3) are the effective relaxation time. The distribution of relaxation times and non-linearity are basic features of the relaxation process. It is best described by the visco-elastic theory. When a stress σ_o is applied during the time period t_1 to t_2 (creep, see Fig. 11), deformation of the material takes place. For an elastic material the deformation is shown by line a (broken line). There is a sudden increase in deformation at time t_1 and the deformation remains constant until time t_2. The viscous material follows the straight line b with gradual change in deformation with time. For the visco-elastic material, the response is represented by a solid line c, i.e. a sudden increase of deformation at time t_1 followed by a further gradual increase until time t_2. When the stress is released at t_2 the deformation decreases immediately to zero for the elastic material, while the deformation remains unchanged for the viscous material. The deformation of the visco-elastic material is featured by a sudden decrease of deformation at time t_2, which corresponds to the elastic

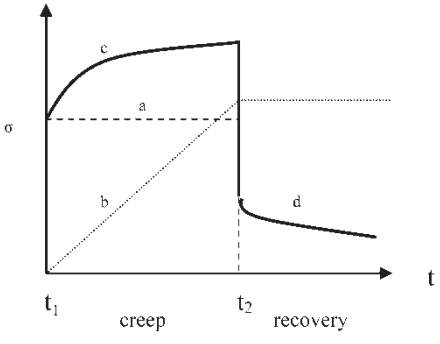

Figure 11. Strain vs. time curve.

component of the material, followed by a further gradual decrease, which-corresponds to the viscous component of the material; as shown in Fig. 11d. The deformation versus time curve after time t_2 is called relaxation or recovery curve, in Fig. 11. Interestingly, a similar relationship was observed between the gas permeation rate and time (10, 11). McCaig et al. (19) ascribed the early steep stage to the dominance of lattice contraction and the later slow stage to the dominance of free volume diffusion mechanism. In other words, lattice contraction corresponds to the elastic component and the free volume diffusion corresponds to the viscous component.

Realizing the resemblance between the gas permeation rate versus the time curve and the visco-elastic response, the data from the gas permeation experiments will be interpreted based on the following assumptions.

1. The relaxation of the polymeric membrane starts from time zero. This assumption may seem unjustified since all membranes have their history of relaxation before being mounted to the permeation cell. The above assumption can, however, be employed, when membranes with the same pre-gas permeation history are compared.
2. The gas permeation rate reflects the visco-elastic response of the glassy polymer; i.e. the initial steep decline in the permeation rate corresponds to the elastic response of the polymer. The following less steep and more linear drop in the permeation rate corresponds to the viscous response of the polymer.
3. The behavior of the polymeric membrane is more elastic when the pressure of the gas that surrounds the membrane is lower, while the membrane's behavior is more viscous when the pressure is higher. Gas, when dissolved in polymer, acts like a solvent that makes the polymer "solution" more like viscous liquid. The higher the gas pressure, the more the polymer "solution" behaves like a viscous solution.

Looking into Fig. 4, Q/Q_0 keeps decreasing for the continuous routine from 20 to 80 hours, where the slope of the curve suddenly changes. The earlier part corresponds to the elastic response, turning later into a viscous response. The steep decrease in Q/Q_0 (elastic response) is more obvious in the non-continuous routine (4-B), when the pressure reduction was applied at the 20 and 40 hours of operation. After 80 hours, a transition in the permeation rate takes place and both response curves become more linear and parallel to each other. The transition occurs suddenly in the continuous routine, while it occurs more smoothly in the non-continuous routine.

In Figs. 5 and 6, we will first look at the curves 5-B and 6-B. Both are experiments of non-continuous routine. During the first 10 hours, no pressure was applied to the feed gas, so the effect is the same as the pressure reduction in the C-P system. The response contains a relatively large amount of elasticity, which is observed as steep decline in the permeation rate. This first stage is followed by a linear decrease where the viscous response dominates. It is

worth noting that the flux reduction during the first 10 hours was more severe for a thinner (5-B) than thicker (6-B) membrane. Now looking into the response curves 5-A and 6-A (continuous routine), the transition from steep to less steep reduction in permeation rate did not occur in the experiment 5-A with a membrane of 5.5 μm during the entire 150 hours of operation while the transition occurred at 30 hours in 6-A, which was with a membrane of 7.25 μm.

The fast appearance of transition for the thicker membrane is one of the important features of the experimental observation. By comparing the lines representing the operating pressure of 25 psig in Figs. 7 and 8 (7-B and 8-B), the transition for 8-B (5.5 μm) occurred much earlier than in 7-B (3.9 μm).

Looking into Fig. 9, the relatively steep decrease in Q/Q_0 observed during the first 1.5 hours is considered to be an enhanced elastic response. Although this turns gradually into the viscous response of less steep decrease both in continuous and non-continuous routines, the decrease in permeation rate seems steeper for the latter operation due to the residual elasticity at the reduced pressure. Eventually, the viscous response of the membrane will dominate after 50 hours and the responses for both continuous and non-continuous routines become parallel.

The effect of the pressure on membrane aging was most clearly observed when the non-continuous routine was applied in the CV system (Fig. 10). It should be recalled that during the pressure reduction period in the CV system, the membrane was under vacuum. The fast decrease in Q/Q_0 has happened during the first 16 hours of the non-continuous routine due to the strong elastic behavior that occurred when the membrane was under vacuum. This is followed by a less steep and more linear response, indicating domination of the viscous component.

CONCLUSIONS

Resemblance of aging curves of gas separation membranes to the visco-elastic response curves is clearly observed for all the studied membranes. Thus, membrane aging curves consist of elastic and viscous components. It is further concluded that the elastic component of polymer relaxation is enhanced when membranes are aged at lower pressures while the viscous component is enhanced at higher gas pressures. It can also be concluded that the transition from the elasticity dominant to the viscosity dominant region occurs more quickly for thicker membranes.

REFERENCES

1. Alfrey, T., Goldfinger, G., and Mark, H. (1943) The apparent second-order transition point of polystyrene. *J. Appl. Phys.*, 14: 700–705.

2. Kauzmann, W. (1948) Nature of the glassy state. *Chem. Rev.*, 43: 219–256.
3. Hirai, N. and Eyring, H. (1958) Bulk viscosity of liquids. *J. Appl. Phy.*, 29 (5): 810–816.
4. Curro, J.G., Lagasse, R.R., and Simha, R. (1982) Diffusion model for volume recovery in glasses. *Macromolecules*, 15: 1621–1626.
5. Hutchinson, M.J. (1995) Physical aging of polymers. *Prog. Sci.*, 20: 703–760.
6. Ramos, A.R., Kovacs, A.J., O'Reilly, J.M., and Greener, J. (1988) Effect of combined pressure and temperature changes on structural recovery of glass-forming materials: 1extension of KAHR model. *J. Appl. Polym. Sci.*, 26: 501–513.
7. Chartoff, R.P. (1997) In *Thermal Characterization of Polymeric Materials*; Turi, E.A. (ed.); Academic Press: New York, pp. 548–573.
8. Tribone, J.J. and O'Reilly, J.M. (1989) Pressure-jump volume-relaxation studies of polystyrene in the glass transition region. *J. Polym. Sci. Part B: Polym. Phy.*, 27: 837–857.
9. Deng, Q. and Jean, Y.C. (1993) Free volume distribution in an epoxy polymer probed by positron annihilation: Pressure dependence. *Macromolecules*, 26: 30–34.
10. Pfromm, P.H. and Koros, W.J. (1995) Accelerated physical aging of thin glassy polymer films: evidence from gas transport measurements. *Polymer*, 36: 2379–2387.
11. McCaig, M.S. and Paul, D.R. (2000) Effect of film thickness on the change in gas permeability of a glassy polyarylate due to physical aging: Part I. Experimental observations. *Polymer*, 41: 629–637.
12. Pinnau, I., Cassilas, C.G., Morisato, A., and Freeman, B.D. (1997) Long-term permeation properties of poly(1-trimethylsilyl-1-propyne) membranes in hydrocarbon—vapor environment. *J. Polym. Sci. Part B: Polym. Phys*, 35: 1483–1490.
13. Nagai, K., Higuchi, A., and Nakagawa, T. (1995) Gas permeability and solubility of poly(1-trimethylsilyl-1-propyne-*co*-phenyl-1-propyne) membranes. *J. Polym. Sci.: Part B: Polym. Phys*, 33: 289–298.
14. Morisato, A., He, Z., and Pinnau, I. (1999) Mixed-gas properties and physical aging of poly(4-methyl-2-pentyne). *ACS Symposium Series*, 733: 56–67.
15. Chung, T.S. and Teoh, S.K. (1999) Aging phenomena of polyethersulfone hollow fiber membranes. *J. Membr. Sci.*, 152: 175–188.
16. Zhou, C., Chung, T.S., Wang, R., and Goh, S.H. (2004) Governing equation for physical aging of thick and thin fluoro-polyimide films. *J. Appl. Polym. Sci.*, 92: 1758–1764.
17. Koros, W.J. and Chern, R.T. (1987) *Separation of Gaseous Mixtures using Polymer Membranes, Handbook of Separation Process Technology*; Rousseau, R.W. (ed.); Wiley.
18. Tabe, M.A., Matsuura, T., and Sourirajan, S. (1995) Design and construction of gas permeation system for the measurement of low permeation rates and permeate compositions. *J. Memb. Sci.*, 98: 281–286.
19. McCaig, M.S., Paul, D.R., and Barlow, J.W. (2000) Effect of film thickness on the change in gas permeability of a glassy polyarylate due to physical aging: part II. *Mathematical model. Polymer*, 41: 639–648.